Available online at www.sciencedirect.com
ScienceDirect
Journal of Power Sources 160 (2006) 645–650
JOURNAL OF POWER SOURCES
www.elsevier.com/locate/jpowsour

# Electrochemical and thermal stability of a siloxane-based electrolyte on a lithium transition metal oxide cathode

Hiroshi Nakahara [a,*], Manabu Tanaka [a], Sang-Young Yoon [a], Steven Nutt [b]

[a] *Quallion LLC, Sylmar Biomedical Park, 12744 San Fernando Rd., Sylmar, CA 91342, USA*
[b] *Department of Materials Science and Engineering, University of Southern California, Los Angeles, CA 90089-0241, USA*

Received 28 December 2005; received in revised form 31 January 2006; accepted 31 January 2006

**Abstract**

The compounds deposited on a lithium transition metal oxide charged in a siloxane-based electrolyte were analyzed by Fourier transformation infrared (FT-IR) spectroscopy and thermal analysis. The decomposition of the siloxane-based electrolyte occurred at voltages above 4.2 V, and the compounds that deposited on the cathode surface consisted of species from both the decomposed siloxane molecule and the electrolyte salt. Differential scanning calorimetry (DSC) profiles of the charged cathode revealed an exothermic peak at 130 °C. The exothermic temperature corresponded to the onset of weight loss of the siloxane-based electrolyte, as revealed in the thermal gravimetry-differential thermal analysis (TG-DTA) diagram. The results indicated that the deposited compounds on the cathode surface and the siloxane-based electrolyte were decomposed at this temperature. Finally, two major exothermic peaks in the DSC profile for the siloxane-based electrolyte occurred at higher temperatures than those for carbonate-based electrolyte, and showed reduced heat flow. The present research suggests that the siloxane-based electrolyte can improve safety of a lithium battery.


*Keywords:* Lithium battery; Siloxane; Cathode; Surface analysis; Thermal stability

## 1. Introduction

Recent reports indicate that siloxane is a suitable electrolyte for lithium polymer battery systems because of the high conductivity relative to other polymer electrolytes [1–4]. For example, polyethylene oxide (PEO) is a well-known solid polymer electrolyte that shows conductivity in the range of $10^{-6}$ to $10^{-7}$ S cm$^{-1}$ [5]. However, the conductivity of the siloxane-based electrolyte exceeds that of PEO by several orders of magnitude, with a value of approximately $10^{-3}$ S cm$^{-1}$ [6].

Because of the intrinsic thermal stability, the siloxane-based electrolyte has emerged as a primary candidate for the development of large lithium batteries for applications such as electric vehicles, in which safety is a prime consideration [6]. In recent work, we investigated the SEI film formation of a carbonaceous material charged in a siloxane-based electrolyte [7–11]. Investigations of the siloxane-based electrolyte with an additive [9], with a modified electrolyte salt [10], and with a different siloxane molecular structure [11] illustrated possible pathways for anode improvements required for the development of lithium batteries for practical use.

A fundamental understanding of the interface region between cathode and anode materials and the electrolyte is necessary in order to improve the safety performance of lithium batteries [12–21]. Nevertheless, there have been relatively few reports of surface analysis of cathode active materials charged in conventional carbonate-based electrolytes [22–24]. The surface of the cathode active material ($LiCoO_2$) charged in propylene carbonate with $LiPF_6$ has been investigated by in situ-infrared absorption spectroscopy (IR) and X-ray photoelectron spectroscopy (XPS) [22–24]. In situ-IR revealed absorption and deposition of propylene carbonate decomposition on $LiCoO_2$ [23]. However, these studies have not determined if substances deposited on the surface of the cathode active material have lithium ion conductive capability. Further investigation is needed to understand the degradation capacity of the cathode active materials after long-term evaluations, such as cycling and/or calendar life.

* Corresponding author. Tel.: +1 818 833 2000/2016; fax: +1 818 833 2001.
*E-mail address:* hiroshi@quallion.com (H. Nakahara).

0378-7753/$ – see front matter © 2006 Elsevier B.V. All rights reserved.
doi:10.1016/j.jpowsour.2006.01.084

In earlier work, we used electrochemical impedance spectroscopy to reveal that the SEI layer existed on the cathode charged in siloxane-based electrolyte [25]. The charge-transfer resistance on the cathode charged in siloxane-based electrolyte was greater than that in carbonate-based electrolyte at all the potential range because of the SEI layer.

In order to commercialize a lithium battery containing a siloxane-based electrolyte, development of both the anode and cathode materials compatible with siloxane-based electrolytes is needed. In the present research, we investigated the cathode surface charged in siloxane-based electrolyte by FT-IR in order to establish the characteristics of compounds formed on the cathode surface. Thermal analysis (DSC and TG-DTA) of the siloxane-based electrolyte with the charged (de-lithiated) cathode powder was performed to determine the thermal stability of the electrolyte with a lithium transition metal oxide. $LiNi_{0.8}Co_{0.15}Al_{0.05}O_2$ was used as a lithium transition metal oxide in this study which has superior performance in terms of overdischarge for a lithium secondary battery [26]. The results reported here establish the electrochemical and thermal stability of the siloxane-based electrolyte.

## 2. Experiment

### 2.1. Siloxane-based electrolyte preparation

The siloxane was synthesized at the University of Wisconsin, and the molecular structure is shown in Fig. 1 and was confirmed by FT-IR and NMR ($^1$H, $^{13}$C, and $^{29}$Si) analyses [27–33]. No impurities were detectable in the siloxanes by FT-IR and NMR analyses. The synthesis method used to prepare the siloxane is described below [27–33].

A dehydrogenation reaction was carried out to generate a siloxane. To a three-necked 100 mL flask, pentamethyldisiloxane (20.0 g, Gelest Inc.) and tri(ethylene glycol) allyl methyl ether (34.1 g, distilled) were added. To this mixture, 100 μL Karstedt's catalyst (3 wt.% solution in xylene) was added, and the reaction solution was heated to 75 °C, and then cooled to room temperature. Samples were collected, and the process of hydrosilylation was followed by $^1$H NMR measurements. After completion of the reaction, the excess tri(ethylene glycol) allyl methyl ether and its isomers were removed by Kugelrohr distillation. A yellowish/brown liquid resulted, and was decolorized by activated charcoal in refluxing toluene. The purified product was obtained by vacuum distillation, and the structure was confirmed spectroscopically.

Lithium bis-oxalo borate (LiBOB; Chemetal GmbH) was dissolved in the siloxane to achieve a 0.8 M concentration, and the electrolyte was a liquid at room temperature. The viscosity of siloxane was 3.8 cP at 25 °C [27]. The conductivity and viscosity of siloxane-based electrolyte were $3.65 \times 10^{-4}$ S cm$^{-1}$ and 18 cP at 25 °C [27], respectively.

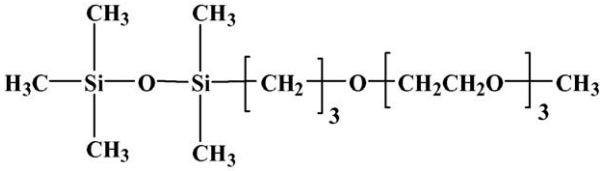


Fig. 1. Structures of the studied siloxane molecule.

### 2.2. Electrochemical cell assembly

The lithium transition metal oxide $LiNi_{0.8}Co_{0.15}Al_{0.05}O_2$ (Toda industry Co., Ltd.) was used as the positive active material and was mixed with a 12 wt.%-solution of PVdF in NMP (Kureha Co., Ltd., PVdF1120), acetylene black and graphite (Timcal Co., Ltd., SFG6) in a mixer. The positive electrode plate was produced by applying the mixed paste to a 20 μm thick aluminum foil using a doctor blade. The coated positive electrode was dried in an oven preset at 120 °C, followed by pressing to 105 μm using a roll press. A 15 mm disk of the positive electrode was cut with a punch, and a lithium metal anode was prepared by punching a 16 mm disk from lithium foil, 0.25 mm thick (Honjo metal Co., Ltd.). Coin cells (2032-type) were prepared by stacking a lithium metal electrode, a separator, a carbonaceous electrode, spacer disks made from stainless steel, and a spring in sequence. The separator was a 25 μm-thick polyethylene porous membrane (Tonen Chemical Co., Ltd.). The separators and electrodes were immersed into each of the siloxane-based electrolytes described above. All parts used for the coin cell assembly were dried in a vacuum oven at 60 °C for more than 8 h. The control electrolyte consisted of ethylene carbonate (EC) and diethyl carbonate (DEC) mixed 50/50 by volume, into which 0.8 M of LiBOB was dissolved.

The electrochemical cells were then charged using constant current at a rate of *C*/10 to 4.3 V, followed by charging at constant voltage until the current fell to *C*/20 at room temperature. The same cells were discharged to 2.7 V at *C*/20 at room temperature in order to investigate the discharge capacity of the electrochemical cell. For FT-IR and DSC measurements of the charged cathode material, the electrochemical cells were charged at *C*/100 to the prescribed voltage (3.85–4.4 V) at room temperature, and then disassembled to remove the cathode for further investigation.

### 2.3. FT-IR measurements

The charged electrochemical cells were disassembled in a glove-box filled with argon gas, and the dew-point was maintained below −75 °C. The cathodes were removed from the cells, rinsed with tetrahydrofuran (THF), and dried under vacuum at room temperature. FT-IR measurements were carried out using a spectrometer (Perkin Elmer Inc., Spectrum One FT-IR spectrometer) installed in a glove-box with argon gas and a dew-point maintained below −75 °C. Electrolyte was squeezed out from a separator, and the FT-IR spectra were measured under the same conditions described above. In addition, FT-IR spectra were acquired from the unused electrolyte to detect any impurities generated by chemical decomposition. This electrolyte was stored in a polypropylene bottle in a glove-box until other sample electrolytes taken from test cells were prepared.

### 2.4. DSC and TG-DTA measurements

The charged electrochemical cells were disassembled, and the charged cathode electrodes were removed. The sample cathode powder was peeled off from the aluminum foil and placed in a stainless steel cell for DSC measurement. DSC measurements were carried out (Perkin Elmer Inc., Pyris 1 DSC) at a heating rate of 5 °C min$^{-1}$ from 20 to 400 °C in flowing nitrogen. Next, the cathode powder charged in the siloxane-based electrolyte was heat-treated at 150 °C for 10 min in the DSC pans, followed by cooling to room temperature. The same DSC measurements as mentioned above were then carried out with the cooled cathode powder to explore the effect of heat treatment on the DSC profiles. Finally, the thermal stability of the siloxane-based electrolyte was investigated using TG-DTA (Perkin Elmer Inc., Diamond TG-DTA). Samples were heated at 5 °C min$^{-1}$ from 20 to 600 °C in flowing argon.

## 3. Results

### 3.1. Electrochemical property

The charge and discharge curves of electrochemical cells fabricated with the siloxane-based and carbonate-based electrolytes are shown in Fig. 2. The discharge capacity of the cell with the siloxane-based electrolyte and a cathode active material was 162 mAh g$^{-1}$, a value nearly identical to the cell with the carbonate-based electrolyte (165 mAh g$^{-1}$). The coulomb efficiency for the cell with siloxane-based electrolyte was 81%, slightly less than the 84% efficiency for the cell with a carbonate-based electrolyte.

### 3.2. FT-IR

The FT-IR spectra for the siloxane-based electrolytes are shown in Fig. 3. One of the electrolyte samples was stored in a glove-box, while the other two were removed from cells charged at 3.9 and 4.3 V. The three FT-IR spectra were identical. In contrast, FT-IR spectra acquired from the cathode electrode charged at the prescribed voltage (3.85–4.4 V) in electrochemical cells revealed distinct differences, as shown in Fig. 4. Additional peaks appeared in the FT-IR spectra for the cathodes charged at potentials greater than 4.2 V. These peaks appeared at 836, 981, 1045, 1090, 1192, 1246, 1357, 1445, 1790, 1799, 2869, 2952, 3298, and 3685 cm$^{-1}$.

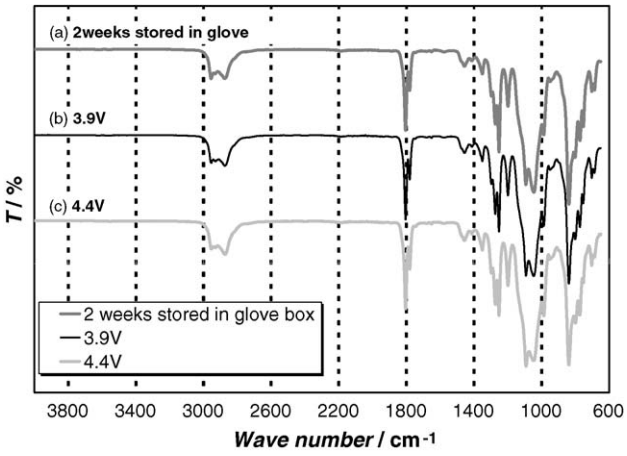


Fig. 3. FT-IR spectra for the siloxane electrolyte: (a) unused control, (b) electrolytes removed from the electrochemical cell charged at 3.9 V, and (c) that at 4.4 V. Lines overlap and show no differences.

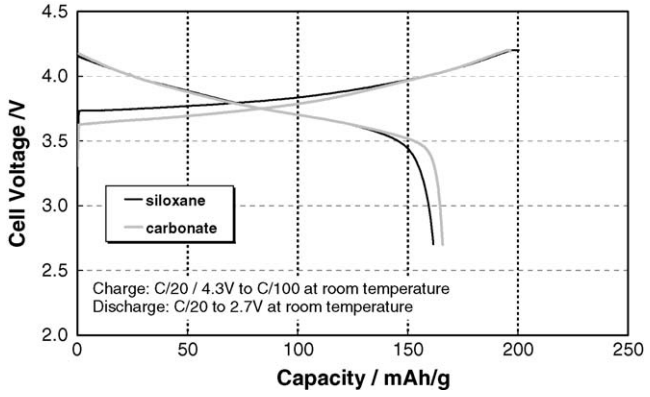


Fig. 2. Charge and discharge curves of the electrochemical cells at the 1st cycle. Capacity is shown for the specific weight of cathode active material.

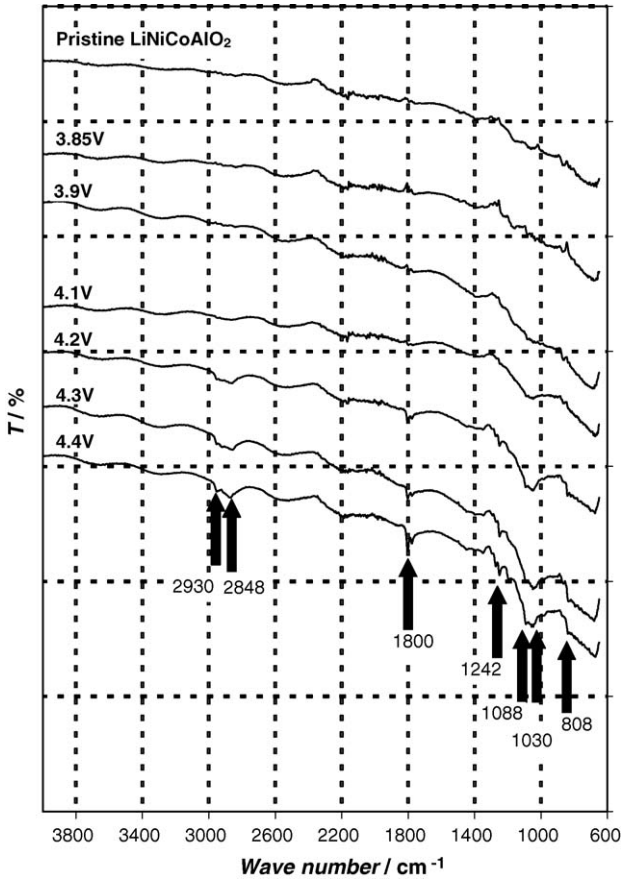


Fig. 4. FT-IR spectra for cathode electrodes charged at different potentials in siloxane-based electrolyte.

### 3.3. DSC and TG-DTA

DSC curves for cathode powders charged in the siloxane-based electrolyte and in the carbonate-based electrolyte are shown in Fig. 5. Three major exothermic peaks were produced (at 195, 230, and 265 °C) by the cathode powder charged in the carbonate-based electrolyte. In contrast, two major peaks were produced by the cathode powder (at 195 and 235 °C) charged in the siloxane-based electrolyte. In addition, the amount of heat flow at 195 °C for the carbonate-based electrolyte was greater than for the siloxane-based electrolyte. Additional major peaks appeared at 230–235 °C for both samples. The peak produced by powder charged in the siloxane-based electrolyte was sharper and at a slightly higher temperature than that for the carbonate-based electrolyte. Furthermore, there was a small peak at 130 °C for the siloxane-based electrolyte.

The effect of heat treatment on the DSC profile of the cathode powder charged in the siloxane-based electrolyte is shown in Fig. 6. The small peak at 130 °C disappeared after heat treatment (at 150 °C for 10 min.). The two major peaks produced by the cathode powder charged in the siloxane-based electrolyte were not affected by heat treatment.

The weight loss during thermogravimetric analysis of the siloxane-based electrolyte (dissolving 0.8 M LiBOB salt) is shown in Fig. 7. The siloxane-based electrolyte decomposed at 132.4 °C until 40% weight loss had occurred. The next weight decrease occurred at 248.5 °C, at which point the sample weight had decreased to 5% of the original weight. The third weight decrement occurred at 473.4 °C, after which 1 wt.% of ash remained.

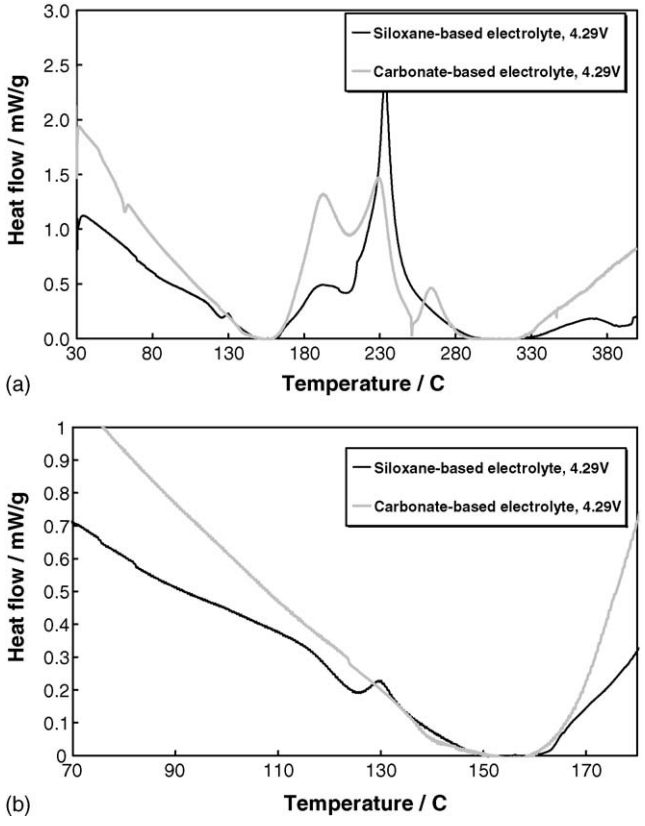


Fig. 5. DSC curves for $LiNi_{0.85}Co_{0.12}Al_{0.3}O_2$ charged in siloxane-based electrolyte and conventional carbonate-based electrolyte: (a) full scale and (b) magnified near 130°.

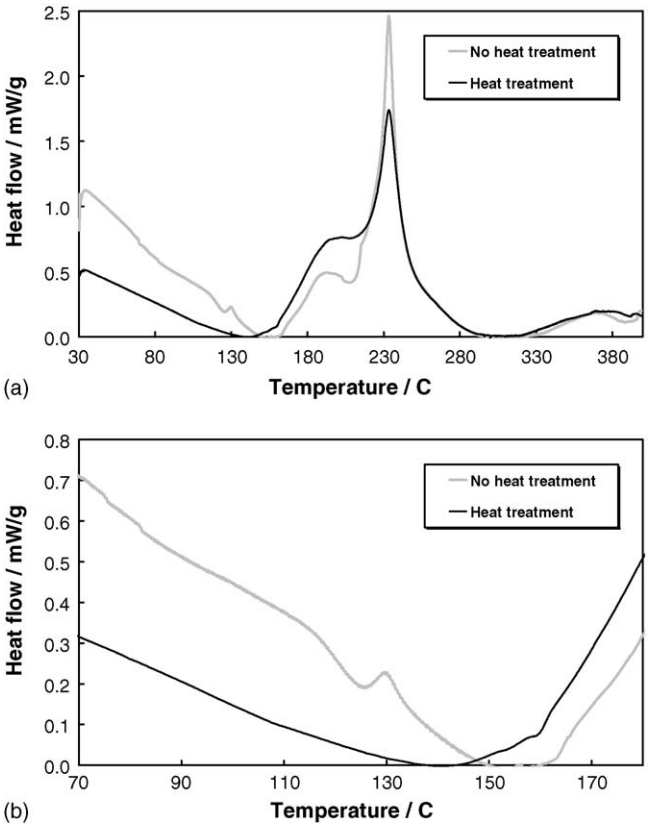


Fig. 6. DSC curves for $LiNi_{0.85}Co_{0.12}Al_{0.3}O_2$ charged in siloxane-based electrolyte with and without heat-treatment at 150 °C: (a) full scale and (b) magnified at 130 °C.

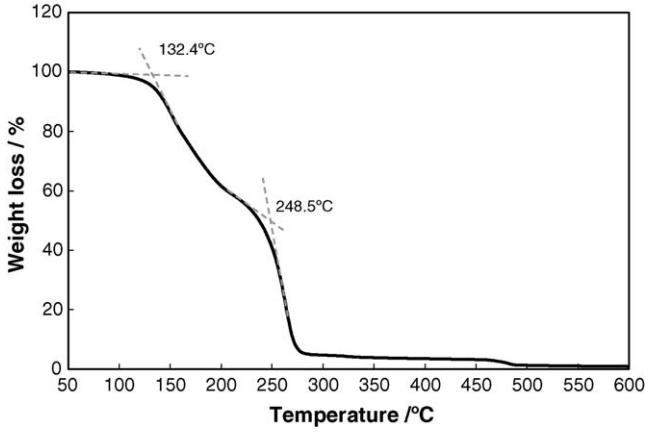


Fig. 7. TG curve for siloxane-based electrolyte containing LiBOB salt.

## 4. Discussion

The cell with the siloxane-based electrolyte demonstrated discharge capacity comparable to the cell with the conventional carbonate-based electrolyte. Taken alone, this suggests that a

siloxane-based electrolyte together with a lithium transition metal oxide is a feasible recipe for an improved lithium battery, at least from the perspective of initial electrochemical characteristics such as discharge capacity. However, the coulomb efficiency of the cell with the siloxane-based electrolyte was 3% less than the cell with the carbonate-based electrolyte, indicating that the additional side reaction(s), such as electrolyte decomposition, occurred in the former electrolyte.

The siloxane-based electrolyte removed from the electrochemical cells charged at 3.85–4.4 V (Fig. 3) showed no signs of the impurity compounds that normally come from electrolyte decomposition on the cathode surface during charging. However, in IR spectra of the cathode powder charged at the prescribed voltage (Fig. 4), the additional absorption peaks appearing after charging at higher voltages (above 4.2 V) indicate the presence of compounds formed by the decomposition reaction of siloxane-based electrolyte and deposited on the cathode surface. These findings indicate that for the present siloxane-based electrolyte, in order to preserve long-term cycling performance and calendar life, the maximum charge voltage for the cathode in the electrochemical cell should not exceed 4.1 V.

The spectral peaks appearing in the IR spectra of the cathode powder charged at higher than 4.2 V (Fig. 4) are assigned to function groups and compounds in Table 1. All peaks are assigned to the function groups that originate from the siloxane molecule and/or LiBOB salt. These assignments indicate that the compounds deposited on the cathode surface were products of the decomposition reaction of siloxane molecules and the LiBOB salt. In addition, all products of siloxane-based electrolyte decomposition at voltages greater than 4.2 V were deposited on the cathode instead of dissolving in the electrolyte. This conclusion is supported by the observation that no impurity was detected in IR spectra from the electrolytes (Fig. 3).

The small exothermic peak at 130 °C in the DSC profile appeared only for the siloxane-based electrolyte. In addition, this peak disappeared after heat treatment of the cathode (Fig. 6). These results support the assertion that the peak at 130 °C arises from combustion of the siloxane-based electrolyte. (The siloxane-based electrolyte control decomposed at 132.4 °C according to the TG-DTA data in Fig. 7.) An alternative possibility is that the peak can be ascribed to combustion of decomposition products having the function groups shown in Table 1. In either case, heat treatment eliminated the peak at 130 °C, indicating that the compound was combusted.

The thermal stability of cathodes charged in the siloxane-based electrolyte was superior to the cathode stability in carbonate-based electrolyte (Fig. 5). This is attributed to the fact that exothermic heat flow at 195 °C for the siloxane-based electrolyte was less than that for carbonate-based electrolyte. In addition, the exothermic peak at 230 °C produced by the carbonate-based electrolyte shifted to a higher temperature when the siloxane-based electrolyte was substituted. These observations indicate that the charged cathode material is more thermally stable in the siloxane-based electrolyte than in the carbonate-based electrolyte.

Table 1
Peak positions in FT-IR spectra from cathode powder charged above 4.2 V, assigned function groups, and possible sources

| Peak position ($cm^{-1}$) | Assigned function groups[a] | Possible source material |
|---|---|---|
| 836 | $SiCH_3$ | Siloxane |
| 981 | C=C | Siloxane or LiBOB |
| 1045 | SiOH, SiOR (SiOSi) | Siloxane |
| 1090 | SiOH, SiOR (SiOSi) | Siloxane |
| 1192 | COOR | LiBOB |
| 1246 | COOR | LiBOB |
| 1357 | $SiCH_3$ | Siloxane |
| 1445 | $SiCH_3$ | Siloxane |
| 1790 | C=O | LiBOB |
| 1799 | C=O | LiBOB |
| 2869 | $SiCH_3$ | Siloxane |
| 2952 | $SiCH_3$ | Siloxane |
| 3298 | SiOH | Siloxane |
| 3685 | C=O | LiBOB |
| 3685 | SiOH | Siloxane |

[a] IR absorption movement of function group is stretching vibration except for C=O (3685 $cm^{-1}$), bending vibration.

## 5. Conclusions

At high charge voltages, the siloxane-based electrolyte decomposed on the cathode surface. In an electrochemical cell, the potential of cathode should not exceed 4.1 V versus $Li/Li^+$ in order to ensure long-term cell performance and to prevent electrolyte decomposition. The compounds formed on the surface of the cathode at high voltage (>4.2 V) resulted from the decomposition of siloxane molecules and the LiBOB salt. This oxidation potential for the siloxane-based electrolyte is comparable to the oxidation potential of the carbonate-based electrolyte [22–24]. The present results thus support the potential for using siloxane-based electrolytes in lithium batteries. In addition, thermal analysis revealed that the siloxane-based electrolyte and the compounds deposited on the cathode surface were decomposed at 130 °C. These data indicate that the safety of a lithium secondary cell can be improved by use of the siloxane-based electrolyte in place of carbonate-based electrolytes.

The siloxane-based electrolyte has potential for use in a commercial lithium rechargeable battery. The discharge capacity of cells based on this electrolyte is comparable to cells with conventional carbonate-based electrolytes, and the batteries are likely to be safer because of the increased thermal stability of the cathode. In future work, the long-term performance characteristics of the siloxane-based electrolyte, such as cycling, self-discharge, and calendar life, will be evaluated.

## Acknowledgements

Financial support from the U.S. Army's Communications-Electronics Research, Development and Engineering Center (CERDEC) is gratefully acknowledged. The University of Wisconsin is acknowledged for preparation of the siloxanes, and technical discussions with personnel at Argonne National Laboratory are gratefully acknowledged.

## References


[1] Y. Kang, W. Lee, D.H. Suh, C. Lee, J. Power Sources 119–121 (2003) 448–453.
[2] I.J. Lee, G.S. Song, W.S. Lee, C. Lee, J. Power Sources 114 (2003) 320–329.
[3] M. Shibata, T. Kobayashi, R. Yosomiya, M. Seki, Eur. Polym. J. 36 (2000) 485–490.
[4] Z. Zhang, S. Fang, Electrochim. Acta 45 (2000) 2131–2138.
[5] Z. Wang, M. Ikeda, N. Hirata, M. Kubo, T. Ito, O. Yamamoto, J. Electrochem. Soc. 146 (6) (1999) 2209–2215.
[6] B. Oh, D. Vissers, Z. Zhang, R. West, H. Tsukamoto, K. Amine, J. Power Sources 119–121 (2003) 442–447.
[7] H. Nakahara, A. Masias, S.Y. Yoon, T. Koike, K. Takeya, Proceedings of the 41st Power Sources Conference in Philadelphia, 14–17 June, 2004, p. 165.
[8] H. Nakahara, S.Y. Yoon, T. Piao, S. Nutt, F. Mansfeld, J. Power Sources 158 (2006) 591–599.
[9] H. Nakahara, S.Y. Yoon, S. Nutt, J. Power Sources 158 (2006) 600–607.
[10] H. Nakahara, S. Nutt, J. Power Sources 158 (2006) 1386–1393.
[11] H. Nakahara, S.Y. Yoon, S. Nutt, J. Power Sources 160 (2006) 548–557.
[12] M. Inaba, Z. Shiroya, Y. Kawatate, A. Funabiki, Z. Ogumi, J. Power Sources 68 (2) (1997) 221–226.
[13] S.-K. Jeong, M. Inaba, Y. Iriyama, T. Abe, Z. Ogumi, Electrochim. Acta 47 (2002) 1975–1982.
[14] R. Mogi, M. Inaba, Y. Iriyama, T. Abe, Z. Ogumi, J. Power Sources 108 (2002) 163–173.
[15] D. Aurbach, E. Zinigrad, Y. Cohen, H. Teller, Solid State Ionics 148 (2002) 405–416.
[16] D. Aurbach, I. Weissman, A. Zaban, P. Dan, Electrochim. Acta 45 (1999) 1135–1140.
[17] D. Aurbach, A. Zaban, Y. Gofer, Y.E. Ely, I. Weissman, O. Chusid, O. Abramson, J. Power Sources 54 (1995) 76–84.
[18] Z. Ogumi, A. Sano, M. Inaba, T. Abe, J. Power Sources 97/98 (2001) 156–158.
[19] K. Xu, S. Zhang, B.A. Poese, T.R. Jow, Electrochem. Solid-State Lett. 5 (1) (2002) A259–A262.
[20] K. Xu, S. Zhang, T.R. Jow, W. Xu, C.A. Angell, Electrochem. Solid-State Lett. 5 (1) (2002) A26–A29.
[21] K. Xu, S. Zhang, T.R. Jow, Electrochem. Solid-State Lett. 6 (6) (2003) A117–A120.
[22] K. Kanamura, S. Toriyama, S. Shiraishi, Z. Takehara, J. Electrochem. Soc. 142 (1995) 1383.
[23] K. Kanamura, S. Toriyama, S. Shiraishi, Z. Takehara, J. Electrochem. Soc. 143 (1996) 2548.
[24] K. Kanamura, S. Toriyama, S. Shiraishi, M. Ohashi, Z. Takehara, J. Electroanal. Chem. 419 (1996) 77.
[25] M. Tanaka, H. Nakahara, S.Y. Yoon, H. Tsukamoto, S. Nutt, Proceedings of the 208th ECS Meeting in Los Angeles, D2-0719P, 2005.
[26] United States Patent 6,596,439, for Lithium-Ion Battery Capable of being discharged to Zero Volts.
[27] H. Nakahara, Study of passive film formation on graphite surface in polysiloxane-based electrolyte for the application of Li secondary battery, PhD Dissertation, University of Southern California, 2006.
[28] R. Hooper, L.J. Lyons, M.K. Mapes, D. Shumacher, D.A. Moline, R. West, Macromolecules 34 (2001) 931.
[29] Z. Zhang, D. Sherlock, R. West, K. Amine, L.J. Lyons, Macromolecules 36 (2003) 9176.
[30] Z. Zhang, N. Rossi, L.J. Lyons, K. Amine, R. West, Polym. Prepr. 45 (1) (2004) 700.
[31] R. West, Z. Zhang, K. Amine, US Patent Appl. Publ. 2004248014, 14 pp.
[32] R. West, Q. Wang, K. Amine, PCT Int. Appl. WO2003083973, 22 pp.
[33] K. Amine, R. West, Q. Wang, B. Oh, D.R. Vissers, H. Tsukamoto, PCT Int. Appl. WO 2003083972, 43 pp.